CONF-831047--132

HEDL-SA--2962-FP

DE84 006345

POST-TEST EXAMINATION OBSERVATIONS FOR THE W-2 SLSF EXPERIMENT

A. L. Pitner
D. E. Smith
G. E. Culley

September, 1983

AMERICAN NUCLEAR SOCIETY

OCTOBER 30 - NOVEMBER 4, 1983

SAN FRANCISCO, CALIFORNIA

HANFORD ENGINEERING DEVELOPMENT LABORATORY
Operated by Westinghouse Hanford Company, a subsidiary of Westinghouse Electric Corporation, under the Department of Energy Contract No. DE-AC14-76FF02710

MASTER

DISCLAIMER

POST-TEST EXAMINATION OBSERVATIONS FOR THE W-2 SLSF EXPERIMENT

A. L. Pitner, D. E. Smith, G. E. Culley
Westinghouse Hanford Company
Hanford Engineering Development Laboratory, Richland, Washington

The W-2 experiment was conducted in the Sodium Loop Safety Facility (SLSF) in the Engineering Test Reactor (ETR) to characterize the failure response of full-length, preconditioned LMFBR fuel pins subjected to slow transient overpower (TOP) conditions. After 26.5 days of steady state operation at representative LMFBR fuel pin power levels, an overpower transient simulating an unprotected FFTF 5¢/s reactivity insertion event was initiated. Disruptive failure of the seven pin bundle occurred at 3.2 times the nominal power level as predicted, but at an axial midplane location rather than the expected upper third level in the center pin. The objectives of the post-test examination (PTE) were to characterize the physical condition of the test assembly following the disruptive failure, and identify any specific circumstances that may have contributed to the unexpected midplane failure response.

1. Test Description

A cross section of the W-2 test section is shown schematically in Figure 1. The seven-pin test bundle was contained in a fluted tube to reduce flow on the outside regions of the outer pins and thereby provide more prototypic thermal/hydraulic conditions for the center (design) pin. The center test pin contained higher enrichment fuel (91% ^{235}U) than the outer pins (43% ^{235}U) to compensate for the radial flux depression across the test assembly that occurs in the ETR. The experiment also provided for bypass coolant flow to better simulate true LMFBR hydraulic conditions. While the test was designed for and pretest calculations predicted an initial upper level failure in the center pin, test instrumentation indicated that failure first occurred in an outer fuel pin at the axial midplane.

2. Neutron Radiography

Following completion of the transient test, the experiment was partially disassembled and neutron radiographed[1] at the Hot Fuels Examination Facility-North (HFEF-N). The radiographs (both thermal and epi-thermal) of the test assembly are shown in Figures 2 through 5. It was evident that severe disruption of the fuel bundle occurred over a ∿10 cm long section near the axial midplane, substantiating the axial midplane failure indication by the test section thermocouples. Failure of the fluted tube was also indicated in the radiographs, as evidenced by molten fuel debris at the bottom of the fuel bundle and sodium filling of the thermal barrier region to a level near the axial midplane. Below the midplane failure site, the fuel bundle appeared to be undisturbed. The upper portion of the fuel bundle, however, was noticeably distorted, or warped. Fuel particulate could be seen dispersed throughout the upper test section.

An interesting feature observable in the neutron radiographs was that a number of intact fuel pellet shell fragments were visible near the midplane gross failure site. These shells, or rinds, were presumably remnants of fuel pellets after the central molten core had been expelled. The fact that these delicate shells remained intact during the major failure event gave testimony to the comparatively nonviolent nature of the failure event itself. These shells were observed to possess very little strength when recovered during the disassembly operation.

3. Disassembly

The general approach taken in disassembling the test train was to cut the assembly in half at the axial midplane location and separately recover test components from the upper and lower sections. The fuel pin bundle from the lower section after removal from the fluted containment tube is shown in Figure 6. The lower extent of the failure region is ∿40 cm above the bottom of the 91.4 cm long fuel column. Below this area, the fuel pins appeared to be in good condition with no detectable cladding breaches in any of the pins.

The fuel bundle in the lower section did exhibit a slight barrel-shaped bow. After further disassembly, the individual pins were photographed against a gridded background to obtain a measure of the bow magnitude. One such photo is shown in Figure 7. The maximum bow measured by this technique was 0.41 cm. It was determined during analysis[2] of thermocouple data (oscillating temperatures) that dynamic bowing of the fuel pins occurred during the transient portion of the experiment. Post-test analyses[2] performed to evaluate the consequences of these temperature oscillations indicated that the associated pin bowing was of great enough magnitude to enter into the plastic deformation domain. The observed permanent bow in these fuel pins appears to verify that this was indeed the case.

As was known from the neutron radiography, the upper test section was substantially more damaged than the lower section. Figure 8 shows that there were multiple failure sites in the fluted containment tube, and that the upper fuel bundle was noticeably warped. The lower ∿5 cm of this section was basically void, with the next ∿5 cm of the test train containing a fused mass of fuel and cladding debris.

The disassembly plan for the upper test section was to cut it into ∿14 cm long segments and attempt to recover fuel pin remnants from each segment individually. A transverse view of the uppermost section (88 cm level) is shown in Figure 9. While all seven fuel pellets were found to be intact and in their proper position at this level, very little evidence of cladding remaining around the pellets could be found. There was considerable redeposition of once-melted cladding on the inner surface of the fluted containment tube. The flow area reduction due to this redeposition was ∿40%, which is approximately sufficient to account for the coolant flow reduction observed following the final TOP test. All the fuel pellets at this level appeared to have a central void, although the voids were filled with cutting debris in some instances.

The fluted tube on this section was slit longitudinally on two sides, 180° apart. Attempts to pry the fluted tube shell halves off the pin bundle,

however, were unsuccessful due to the excessive fusion of components that occurred at this level. Figure 10 shows a side view of this section after repeated attempts to pry it apart. The cladding in the lower ∿2 cm portion of the fuel pin visible here appeared to be melted away. The upper portion of this section where the inconel reflectors were located appeared to be in good condition, with no apparent fusion of components. The lower portion where the fuel was located, however, displayed extensive fusion of fuel pin cladding with molten fuel debris interspersed throughout the area.

Based on the observations of the uppermost section condition, no further attempts were made at recovering individual pin segments in the remaining portion of the upper test section. Instead, it was decided to obtain metallography specimens of the pin bundle at selected locations. These sections were vacuum impregnated with a resin to fix internal components in place during cutting operations. A transverse view of the pin bundle at the 70 cm level is shown in Figure 11. As observed in the previous section, the cladding was again totally melted away, but the fuel pellets were basically intact and located in their proper positions within the fluted tube. Some deposition of melted cladding on the interior fluted tube wall was evident. The pellets generally showed large central voids where molten fuel had escaped. Molten fuel and cladding residues were interspersed in the flow channels around the fuel pellets. In general, this physical situation was found to prevail from the ∿55 cm level up to the top of the fuel column. The intact, free standing fuel pellet columns in the upper levels of the test section are considered additional testimony to the relatively non-violent nature of the overall failure event.

4. Fuel Expulsion

Based on observations of residual fuel content at various levels in the test section, it was possible to estimate the amount of fuel expelled along the fueled length of the test assembly. Histograms constructed by interpolating between measured points are shown in Figure 12. The outer pin histogram represents the average of the six circumferential pins. These

distributions should represent an upper limit to actual fuel expulsion, since they do not acknowledge localized plugging of the central voids which was observed at several locations. The integrated distributions in Figure 12 indicate that 45.9 g of fuel was expelled from the center pin, and an average of 55.8 g of fuel was expelled from each of the outer pins. These quantities represent 27% and 34% of the fuel loading in the inner and outer pins, respectively. The total quantity of fuel expelled is thus inferred to be 380 g, or 33% of the test bundle fuel loading. This is an approximate estimate due to the basic inaccuracies involved in obtaining these values, but it should represent an upper limit to fuel expulsion as noted above. The 380 g value obtained here is a factor of 2.3 greater than the estimated fuel dispersion obtained from the Delayed Neutron Detection (DND) System (165 g). However, measurement of fission product activity (^{87}Br) in the SLSF after the transient test suggested that more than 165 g of fuel had been dispersed. In actuality, it is felt that the true fuel expulsion value lies somewhere between these two extremes of 14% and 33%. There was substantial upward sweep-out of the fuel expelled at the midplane failure site, as evidenced by fuel debris present in the coolant channels of upper level metallography sections, and fuel particulate matter above the fueled section detectable in the neutron radiographs.

5. Axial Power Profile

In order to obtain an indication of the axial power profile in the test section, gamma scanning was performed on a hardware component from the W-2 test train. The component selected was a stainless steel flow tube for a fission chamber that was located adjacent to the fuel pin bundle. This article was selected because it was uniform along its length and could be easily cleaned of fuel debris.

The isotope activities measured in the steel flow tube were ^{54}Mn and ^{60}Co. The ^{54}Mn activation results from fast neutron captures ($\sim$2-MeV threshold energy) in the iron, and should reflect the axial profile of the fission source. The ^{60}Co activation results from slow neutron interactions with

cobalt impurities in the steel, and accordingly provides an indication of the axial profile of low energy neutrons. These profiles, therefore, should reflect the axial power distribution in the test fuel bundle.

The axial profiles determined from these two isotope activities agreed well (within ~5%) with one another, and their average is shown in Figure 13 along with the predicted axial power profile based on pretest critical facility (ETRC) measurements and neutronic calculations. Each curve has been normalized to an average value of unity over the length of the fuel column. The measured profile is considerably more peaked than the predicted profile, with a peak-to-average (P/A) value of 1.39 for the measured, versus 1.25 for the predicted profile. The measured profile is also seen to be skewed more toward the bottom of the core relative to the predicted profile.

The measured profile with a P/A value of 1.39 is actually very near that of an unperturbed ETR core. In an attempt to achieve a more prototypic LMFBR axial power profile (P/A ≈ 1.25), a number of flux-shaping devices were employed in this ETR test. Hafnium elements were placed in a number of surrounding core positions to suppress the thermal flux component near the axial midplane. Also, a tapered stainless steel collar was affixed to the outside of the test fuel bundle to flatten the incident thermal flux profile an additional small amount. Unfortunately, it would appear that the desired overall flattening of the axial power profile in the test bundle was not achieved. The reason for this anomaly is not known. Pretest ETRC measurements with mock-up components and neutronic calculations indicated that the flux tailoring devices should reduce the P/A value of the axial power profile to ~1.25, and such a large discrepancy between ETRC and ETR measurements is unprecedented. Nonetheless, there is no reason to doubt the validity of the measured gamma scanning profile. In addition, measured fuel bundle temperature data and the observed better-than-expected power coupling between the experiment and the reactor support the more peaked axial power profile.

The principal ramification of the more peaked power profile is that the thermal flux incident on the test assembly was greater than anticipated.

Due to the high efficiency of thermal neutrons in producing fissions, disproportionately more power was produced in the outer test pins than expected, and radial power gradients would have been more severe than calculated in the pretest analyses. This affected the melt zones in the outer fuel pins, as discussed in the next section.

6. Metallography

A number of metallography specimens were taken from the intact lower pin segments. Figure 14 shows a specimen taken from the center pin at the 31 cm level. The various zones progressing from the center out are central void where molten fuel has escaped, resolidified once-molten fuel, restructured (equiaxed grains) fuel, unrestructured fuel, and the stainless steel cladding. The zones are located concentrically around the center of the pin, as would be expected for this central fuel pin. Several radial cracks are present in the specimen, but there was no penetration of molten fuel through the solid outer pellet shell. The beta-gamma autoradiograph of this specimen is shown in Figure 15. This image reflects the fission product distribution in the specimen, which presumably corresponds to the burnup or power distribution within the pellet. The darkness intensity perceptibly decreases as one progresses inward from the outer surface, reflecting the radial power gradient that was prevalent in this thermal reactor test. Another observable feature is that the once-molten fuel annulus is uniform in intensity, and less intense than the surrounding solid fuel pellet. This suggests that the once-molten fuel at this location was relocated from lower elevations (lower burnup) after mixing.

Figure 16 presents an outer pin metallography specimen at the 16 cm level. The fluted tube side of this specimen was toward the two o'clock position. The central void and melt annulus are noticeably skewed in that direction, as a result of the steep radial power gradient through this pin. Two occasions of molten fuel penetration through the solid outer fuel shell are noted in this specimen, although there was no perceptible cladding

melting at the contact points. The beta-gamma autoradiograph shown in Figure 17 again reflects the large radial power gradient through this outer fuel pin.

In general, it was noted in the 13 metallography specimens examined that molten fuel penetration to the cladding occurred once the melt radius exceeded ∿75% of the pellet radius. The penetration usually was in the outward (towards fluted tube) direction. While generally no cladding melting was observable at the point of molten fuel contact, one exception was noted. Figure 18 shows an outer pin specimen taken at the 39 cm level, which is somewhat higher (hotter coolant) than the previous specimen elevations. Once again the central void and melt annulus in this outer pin specimen are offset toward the fluted tube side. A finger of molten fuel penetration on the fluted tube side in this case, however, actually caused some localized melting of the cladding at the inner surface, as depicted in the enlarged views of the etched cladding in Figure 18. The extent of melting was ∿25% of the cladding thickness. On the opposite side of the specimen, an even larger finger of molten fuel penetrated to the cladding, but caused no melting of the cladding. This is because the cladding was cooler at this azimuthal location. It is known from test thermocouple data that coolant temperatures in the outside flow channels reached higher levels than the inboard channels. This has been interpreted[2] to be a result of flow restrictions that occurred in the containment tube flutes as the outer fuel pins bowed into them. Thus it is evident that molten fuel penetration can cause localized cladding melting if cladding temperatures are high enough.

7. Failure Mechanism

While cladding temperatures at the lower elevations where the metallography specimens were procured were low enough to resist failure, this was probably not the case near the axial midplane. Measured thermocouple data indicated that the bowing-induced coolant temperature oscillations were greatest at this location, and that coolant temperatures probably exceeded 1100 K here on oscillation peaks in the latter stages of the overpower

transient. Additionally, it is inferred from lower-level metallography specimen examinations that the extent of fuel melting in some of the outer pins exceeded 90% of the pellet radius near the axial midplane at the end of the transient. These combined conditions (>90% melt radius and >1100 K coolant temperature) are considered sufficient to produce fuel penetration to (and melting of) the cladding, pin failure, and fuel expulsion. This is considered to have been the dominant failure mechanism operative in the initial W-2 midplane failure event. Subsequent rupturing of the fluted duct tube and blanketing of the fuel bundle with the surrounding fill gas (argon) is believed responsible for the melting of cladding observed in the upper half of the fuel bundle.[2]

8. Conclusions

Results obtained from the post-test examination of the W-2 SLSF experiment were instrumental in interpreting the causes and consequences of the unexpected midplane failure experienced in the test. Gamma scanning measurements revealed that the axial power profile in the test trains was more peaked than expected based on pretest calculations and critical facility measurements. These results implied that the thermal flux incident on the test assembly was greater than expected, which was manifested in highly skewed and extensive fuel melting zones in the outer pin fuel pellets. Observations indicated that the extent of fuel melting near the midplane exceeded 90% of the pellet radius in some of the outer fuel pins toward the end of the overpower transient, with penetration of molten fuel to the cladding inner surface. It is postulated that this extensive fuel melting and penetration combined with bowing-induced high temperature oscillations to produce the initial disruptive failure in an outer pin at the midplane. Subsequent failure events were induced by the inrush of argon fill gas following rupture of the fluted duct tube. Up to one-third of the total fuel inventory was expelled from the test pin bundle into the coolant channels, with substantial upward sweepout of the ejected fuel noted in the post-test examination. The overall nature of the failure event was judged

to be relatively non-violent, based largely on the survival of unclad, free standing fuel pellet columns in the upper levels of the test section.

The observed midplane failure in the W-2 experiment has been attributed to conditions unique to the test. These conditions would not exist in full-size LMFBR fuel assemblies, for which fuel pin failure under slow, unprotected TOP conditions would be expected by a different mode at a higher elevation.

References

1. J. M. Henderson et al., Fuel Pin Behavior Under Slow Overpower Transient Conditions; HEDL W-2 Experiment Results, Proc. ANS Top Mtg. on Reactor Safety Aspects of Fuel Behavior, pp. 2-67 - 2-78, Sun Valley, Idaho, August 2-6, 1981.

2. D. E. Smith et al., Post-Test Analysis of the W-2 SLSF Experiment, 1983 ANS Summer Mtg., Detroit, Michigan, June 12-17, 1983.

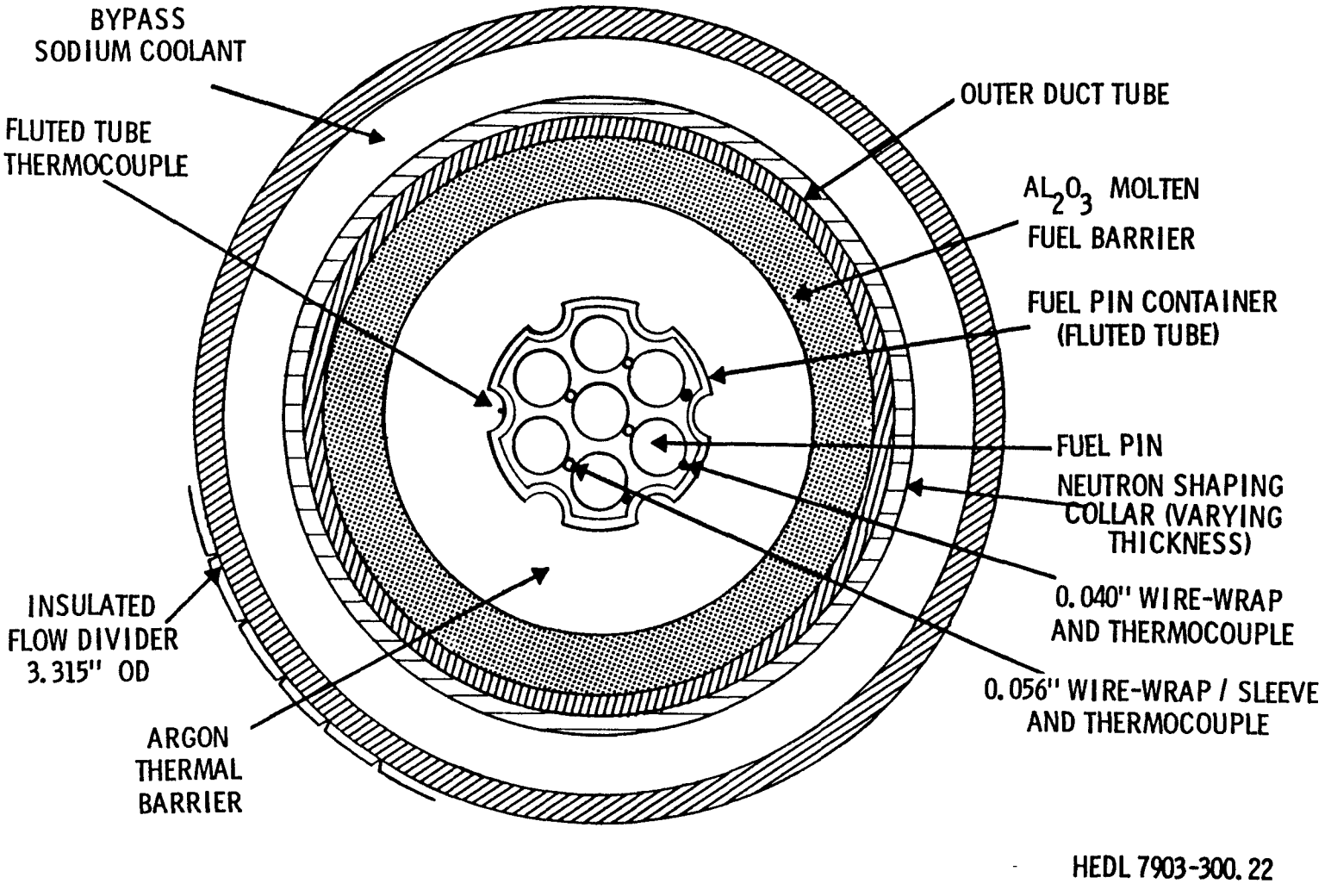

FIGURE 1. Cross-Section of W-2 Test Section.

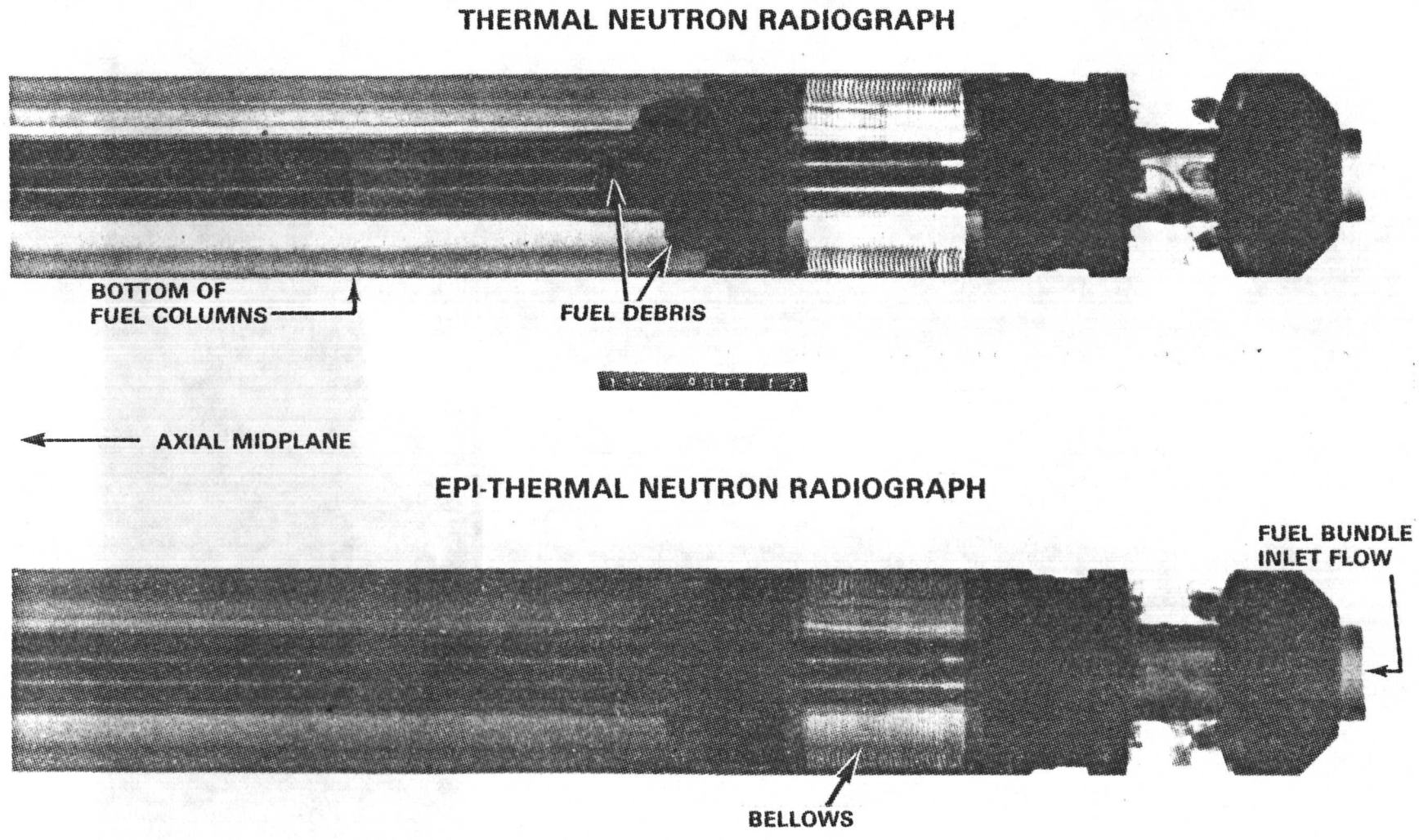

FIGURE 2. Neutron Radiographs of Bottom of Test Section.

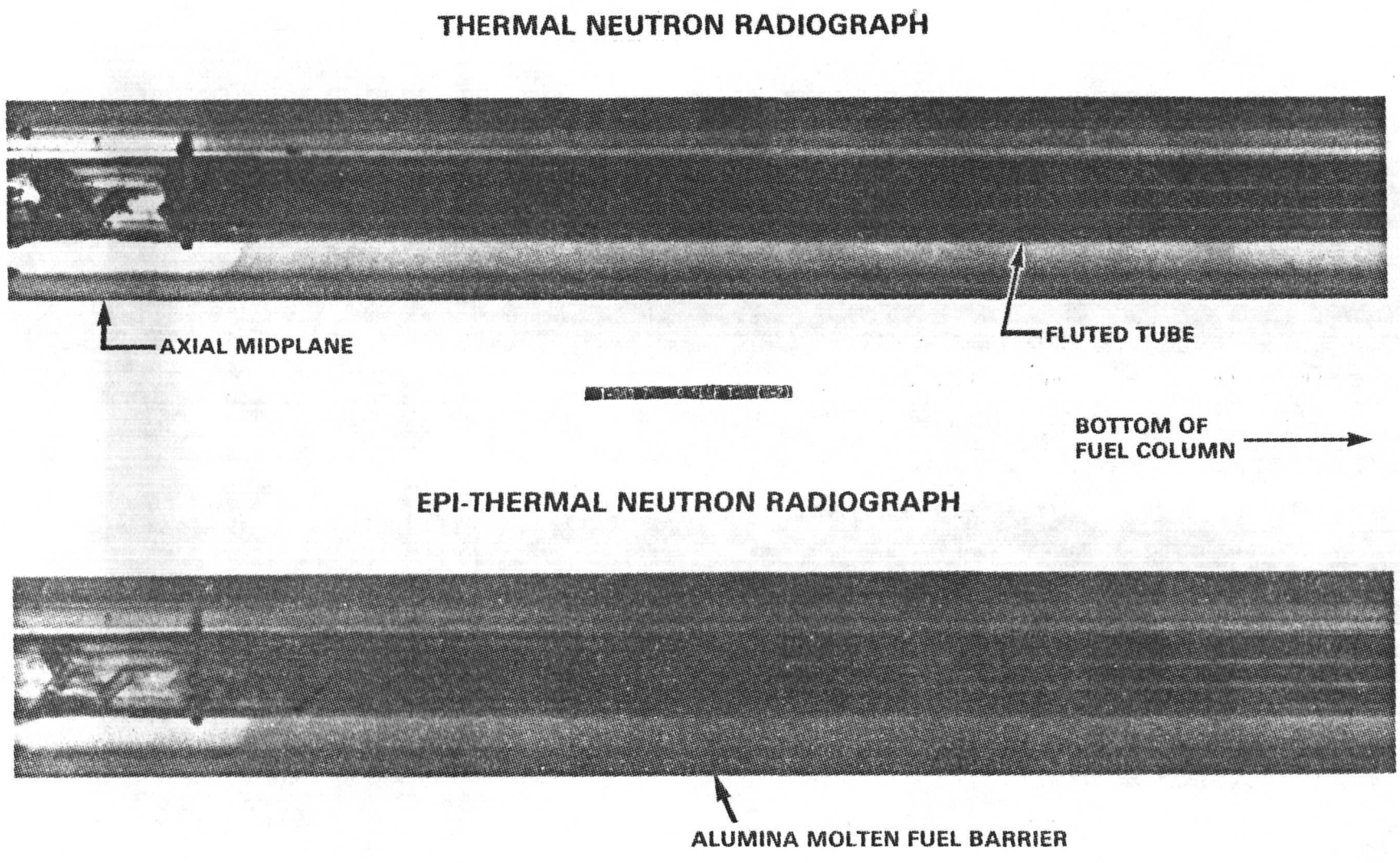

FIGURE 3. Neutron Radiographs of Below-Midplane Test Section.

W-2 ABOVE-MIDPLANE SECTION

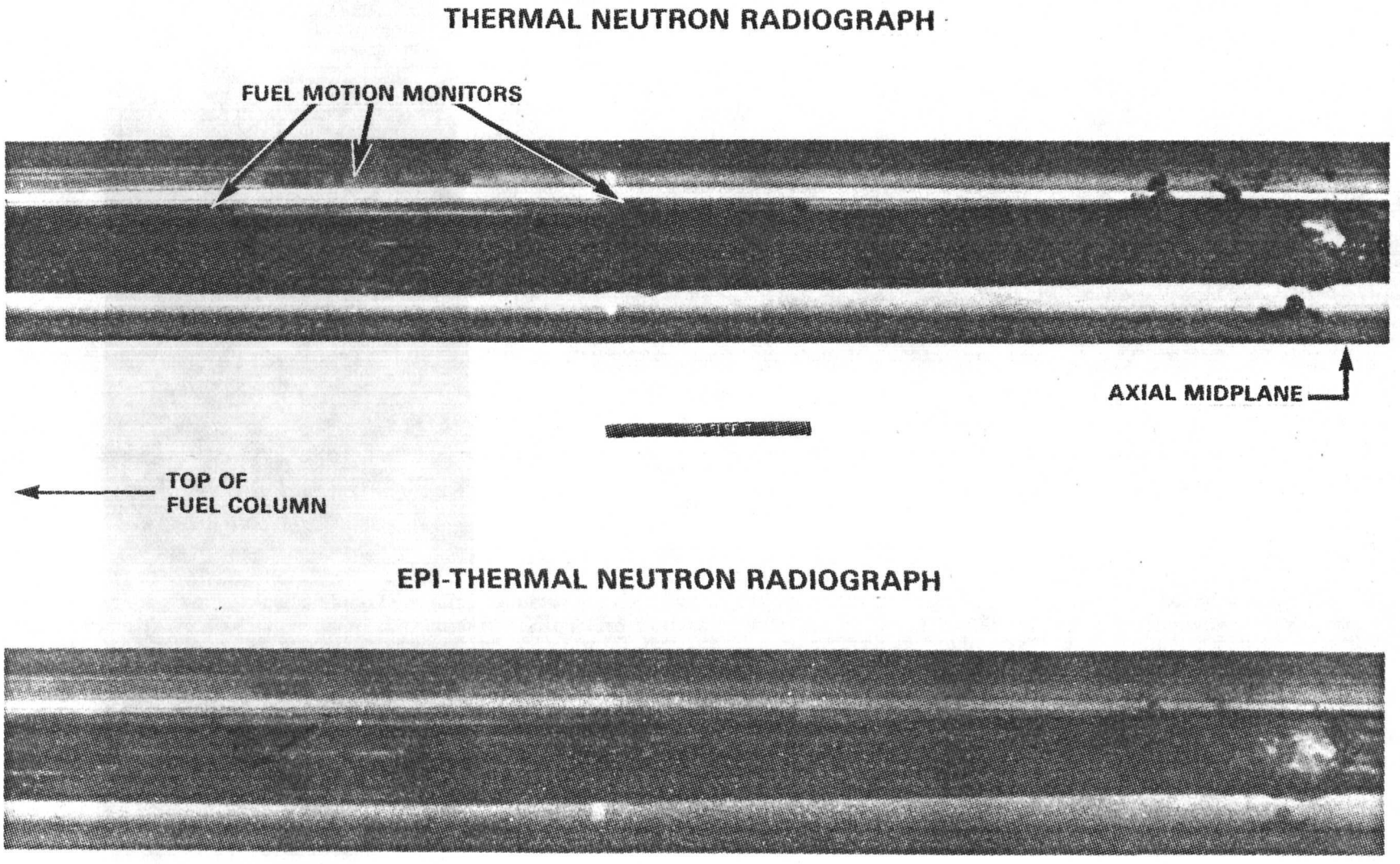

FIGURE 4. Neutron Radiograph of Above-Midplane Test Section.

W-2 TOP SECTION

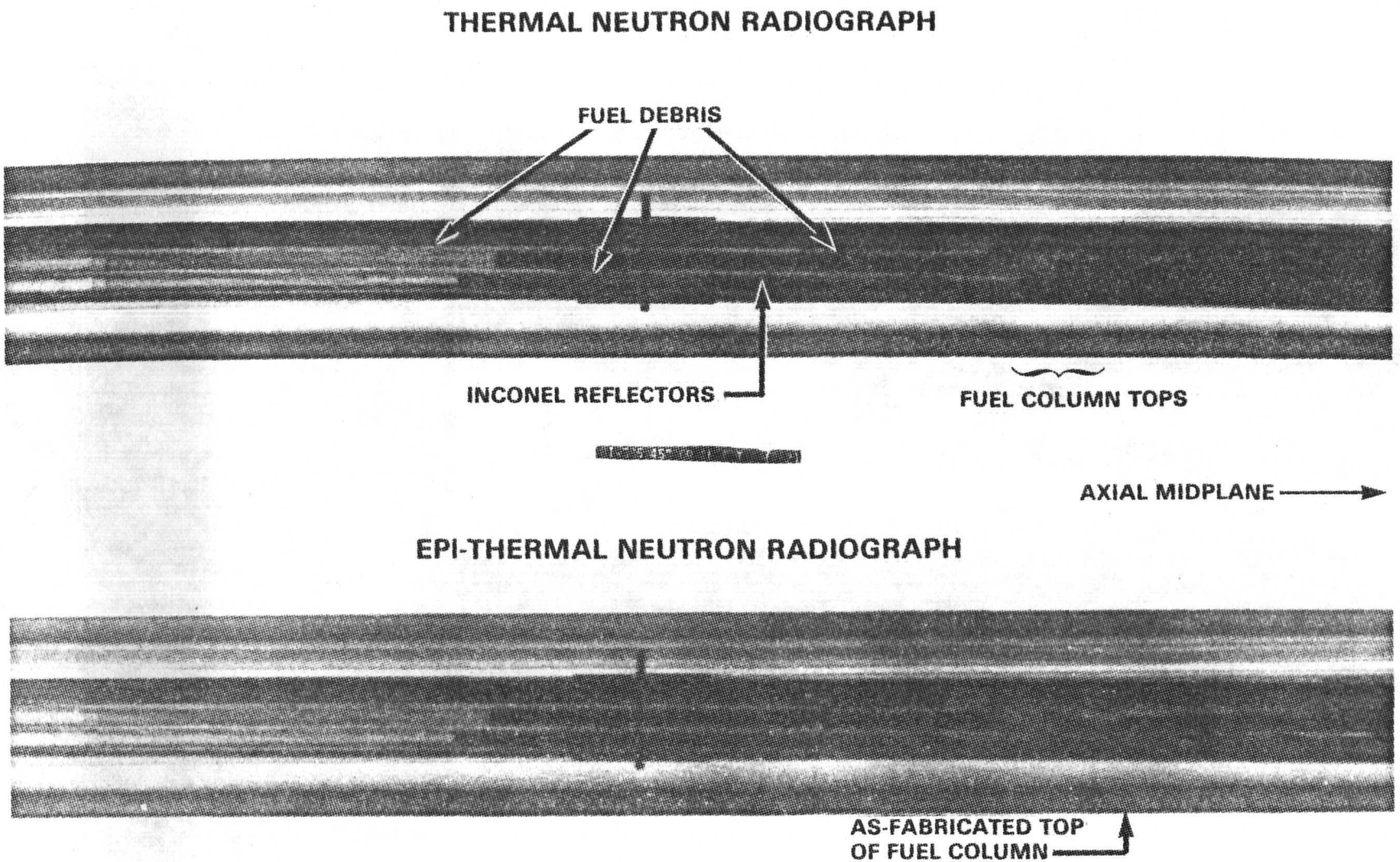

FIGURE 5. Neutron Radiograph of Top of Test Section.

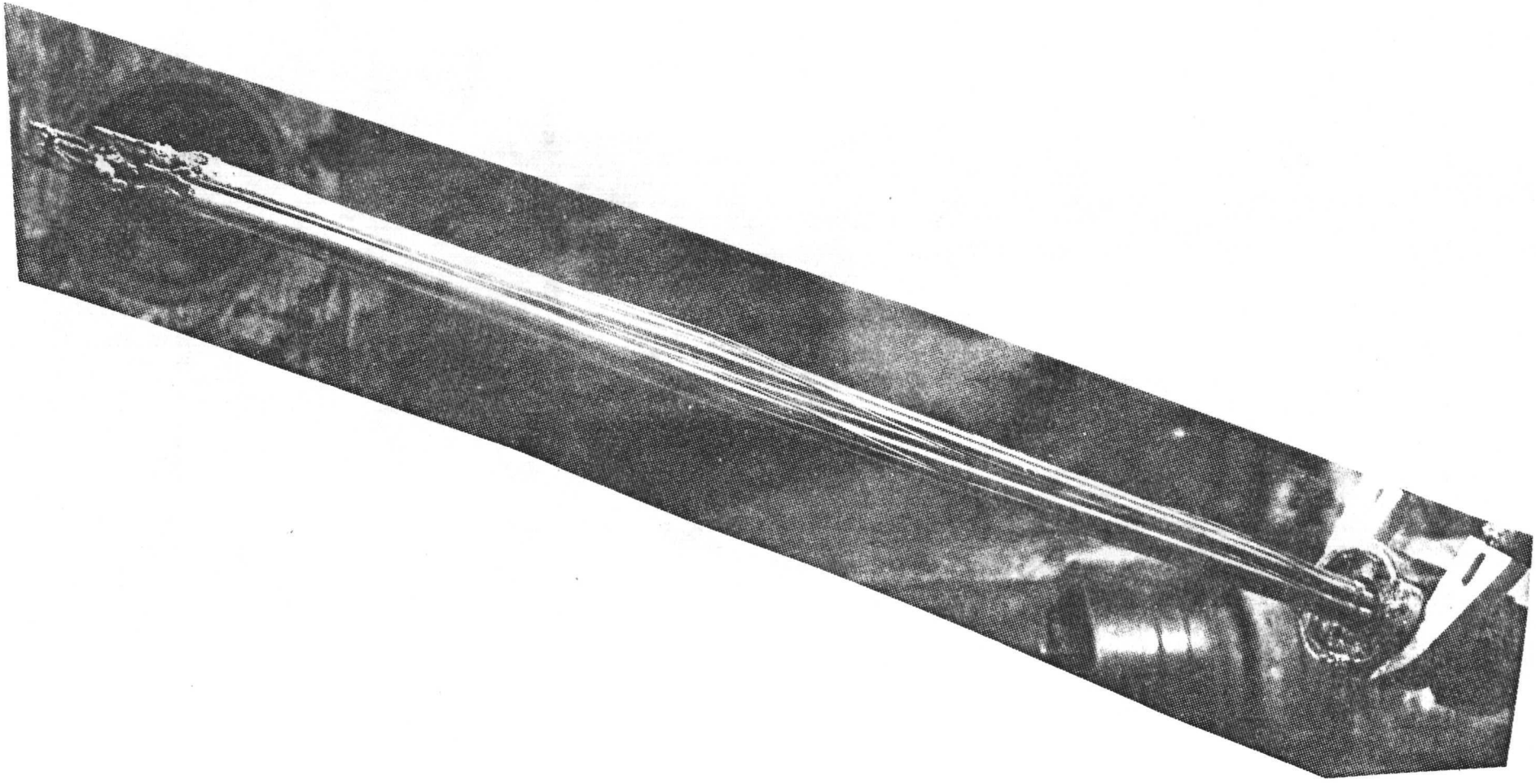

FIGURE 6. Fuel Pin Bundle in Lower Test Section.

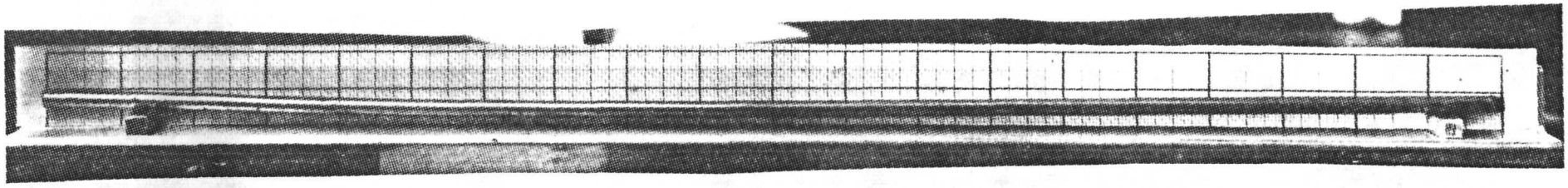

FIGURE 7. Bowing Measurement in a Lower Pin Section.

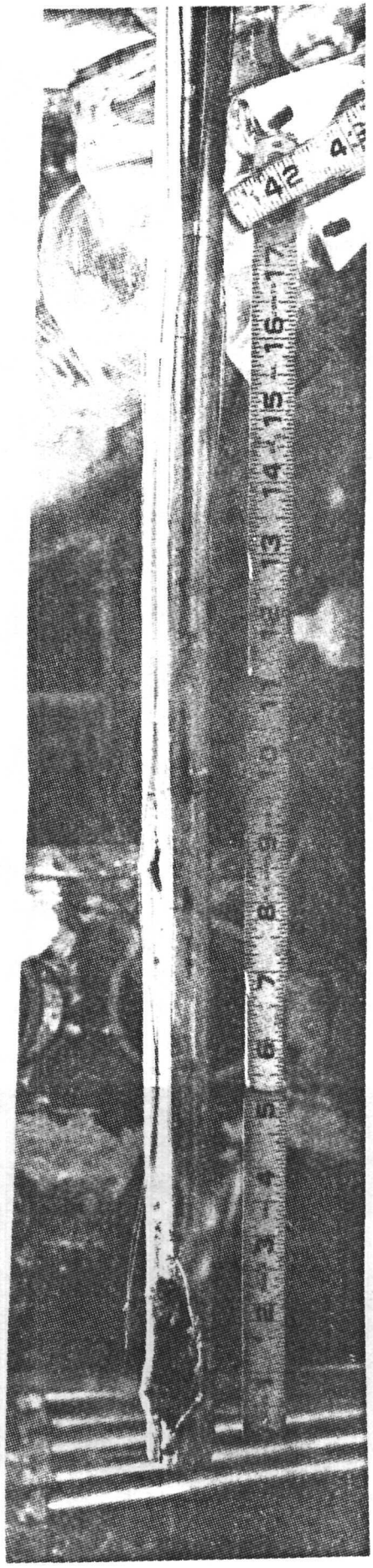

FIGURE 8. Upper Test Section.

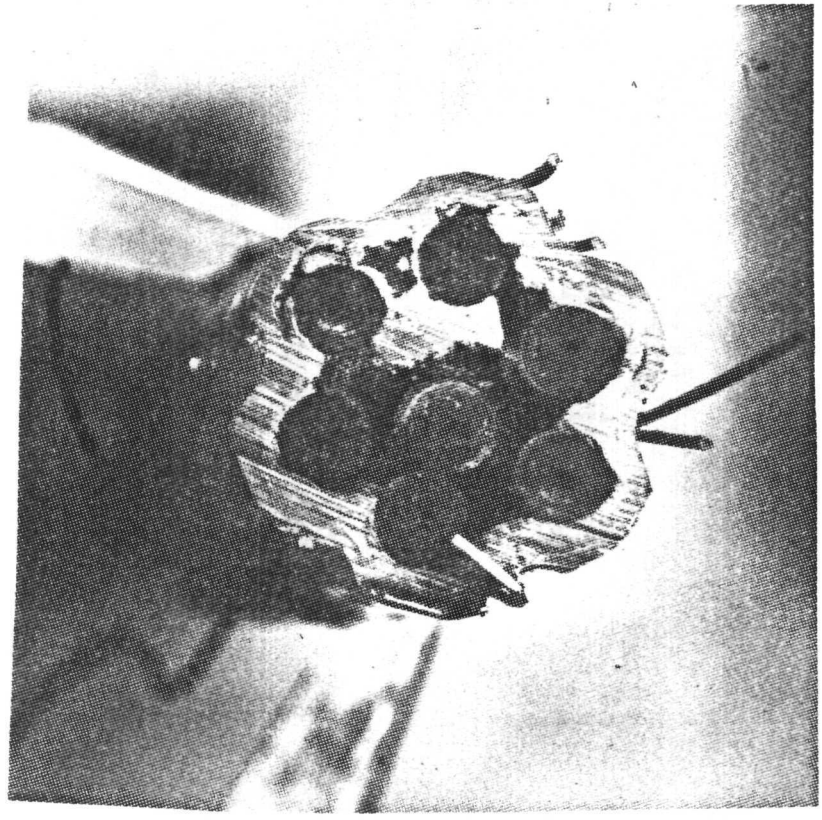

FIGURE 9. Transverse Section of Fuel Pin Bundle at 88 cm Level (Looking Up).

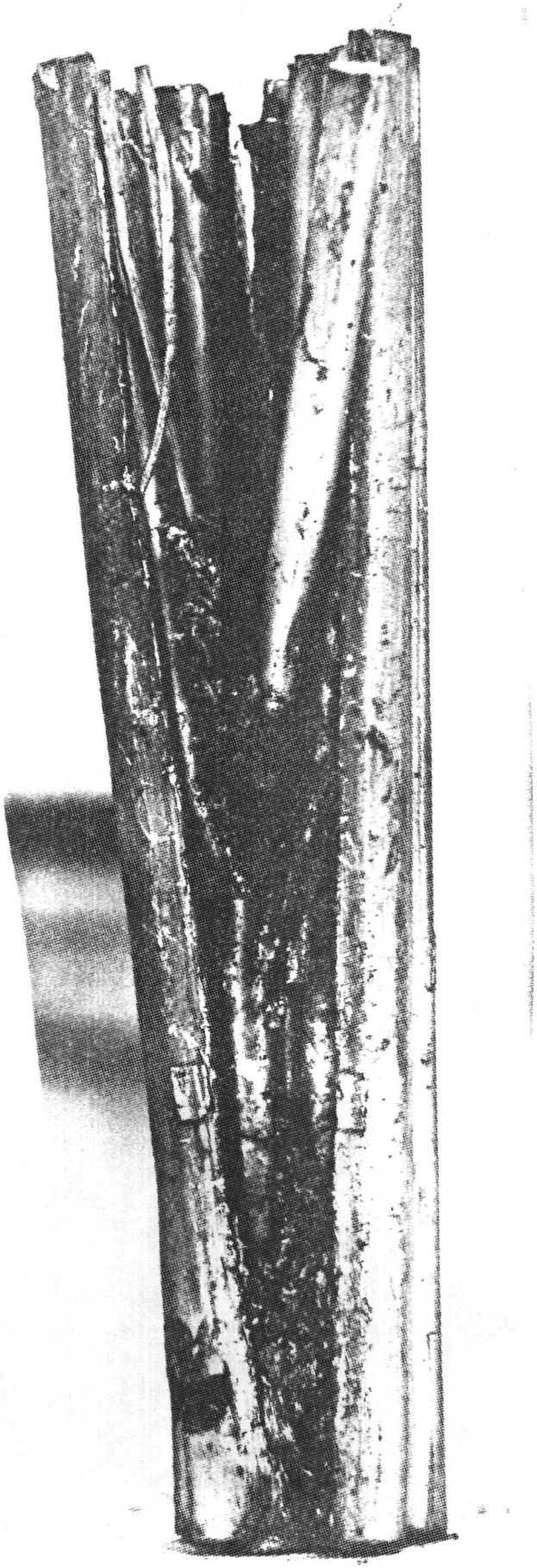

FIGURE 10. Topmost Section of the Fuel Pin Bundle.

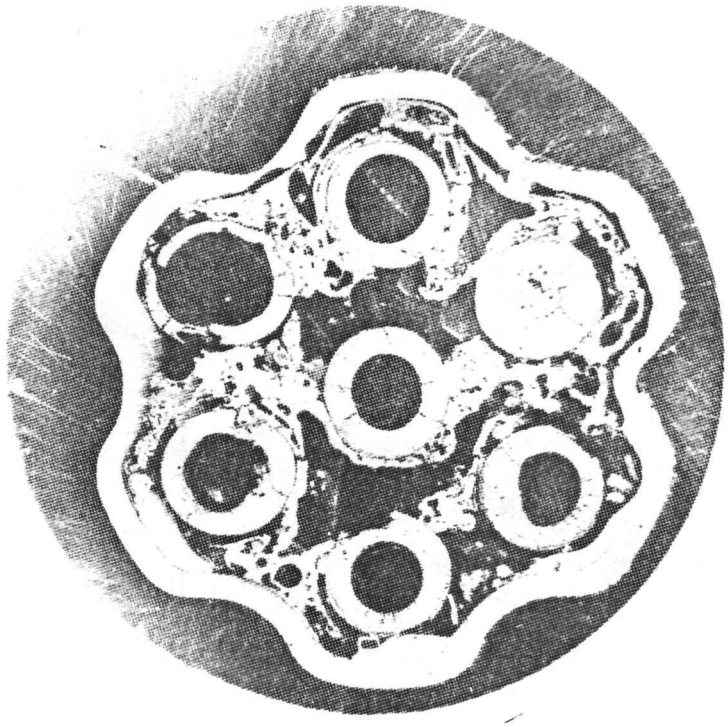

FIGURE 11. Transverse Section of Pin Bundle at the 70 cm Level.

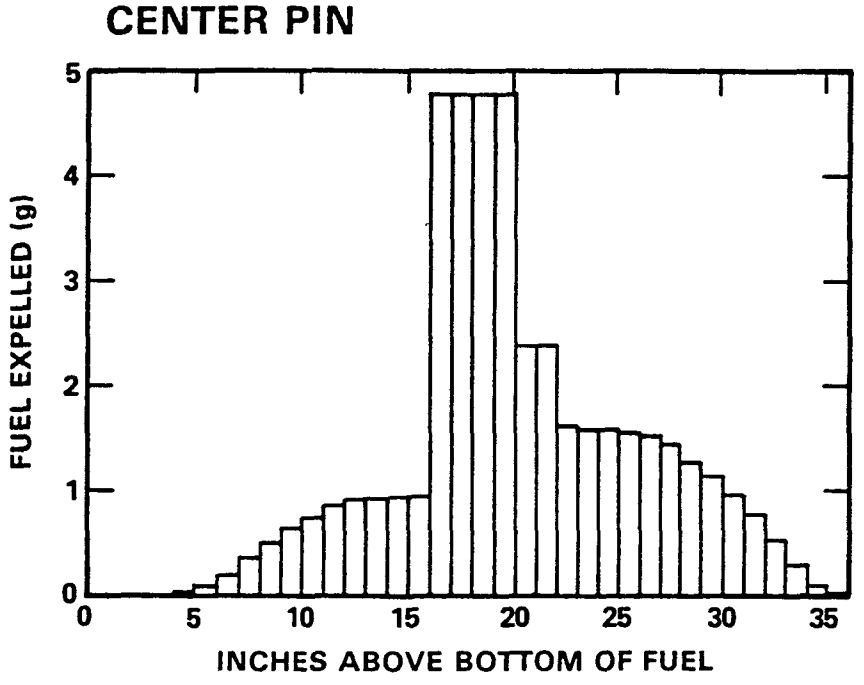

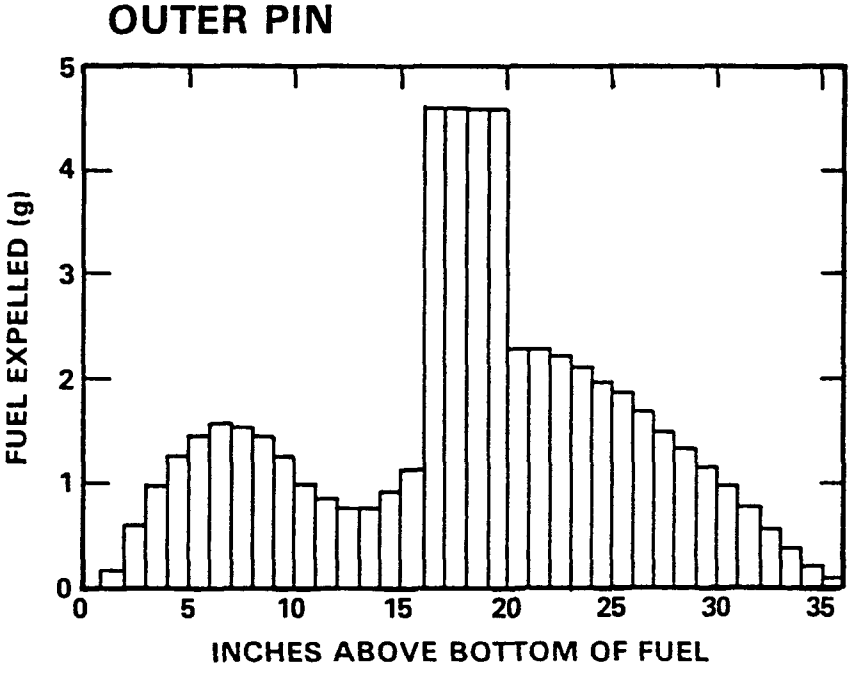

FIGURE 12. Estimated Fuel Expulsion from W-2 Pin Bundle.

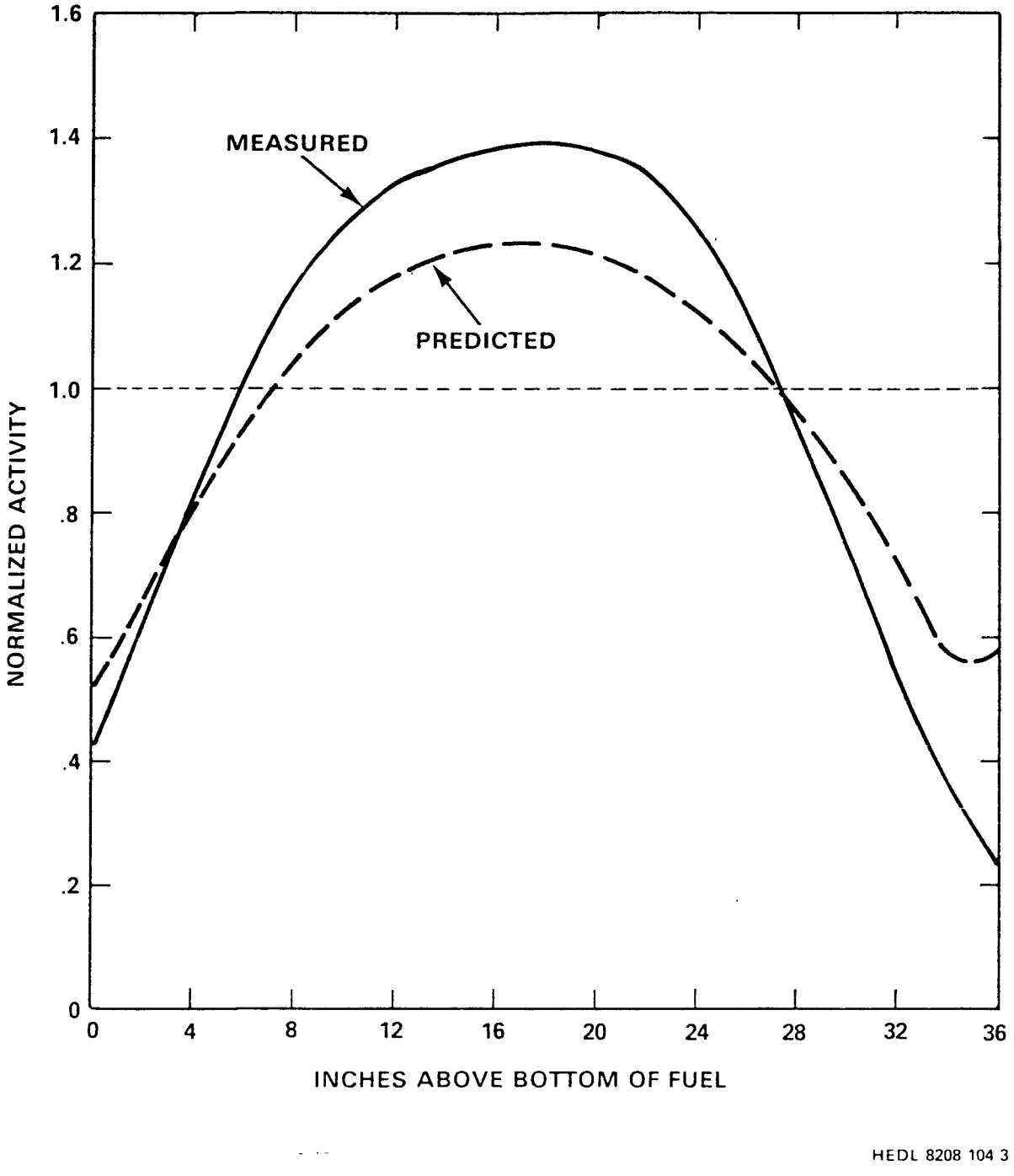

FIGURE 13. Measured Gamma Scan Profile vs. Predicted Profile.

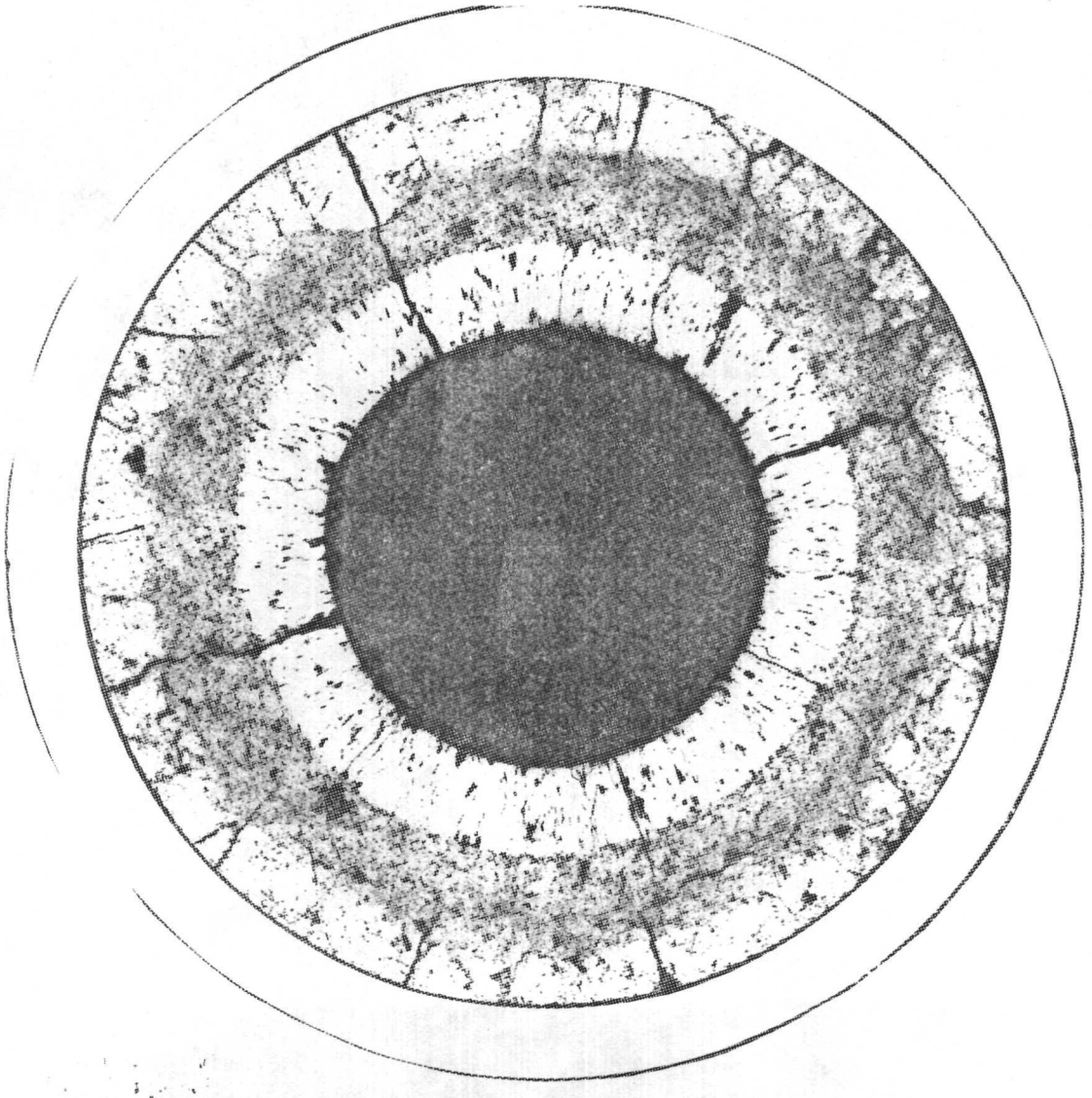

FIGURE 14. Center Pin Specimen at the 31 cm Level.

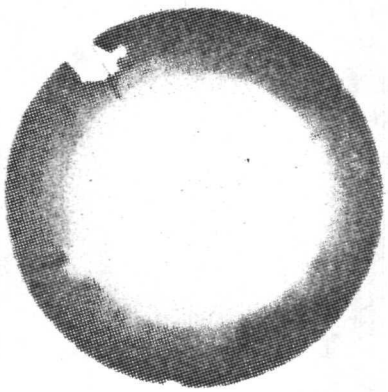

FIGURE 15. Beta-Gamma Autoradiograph of Center Pin Specimen at the 31 cm Level.

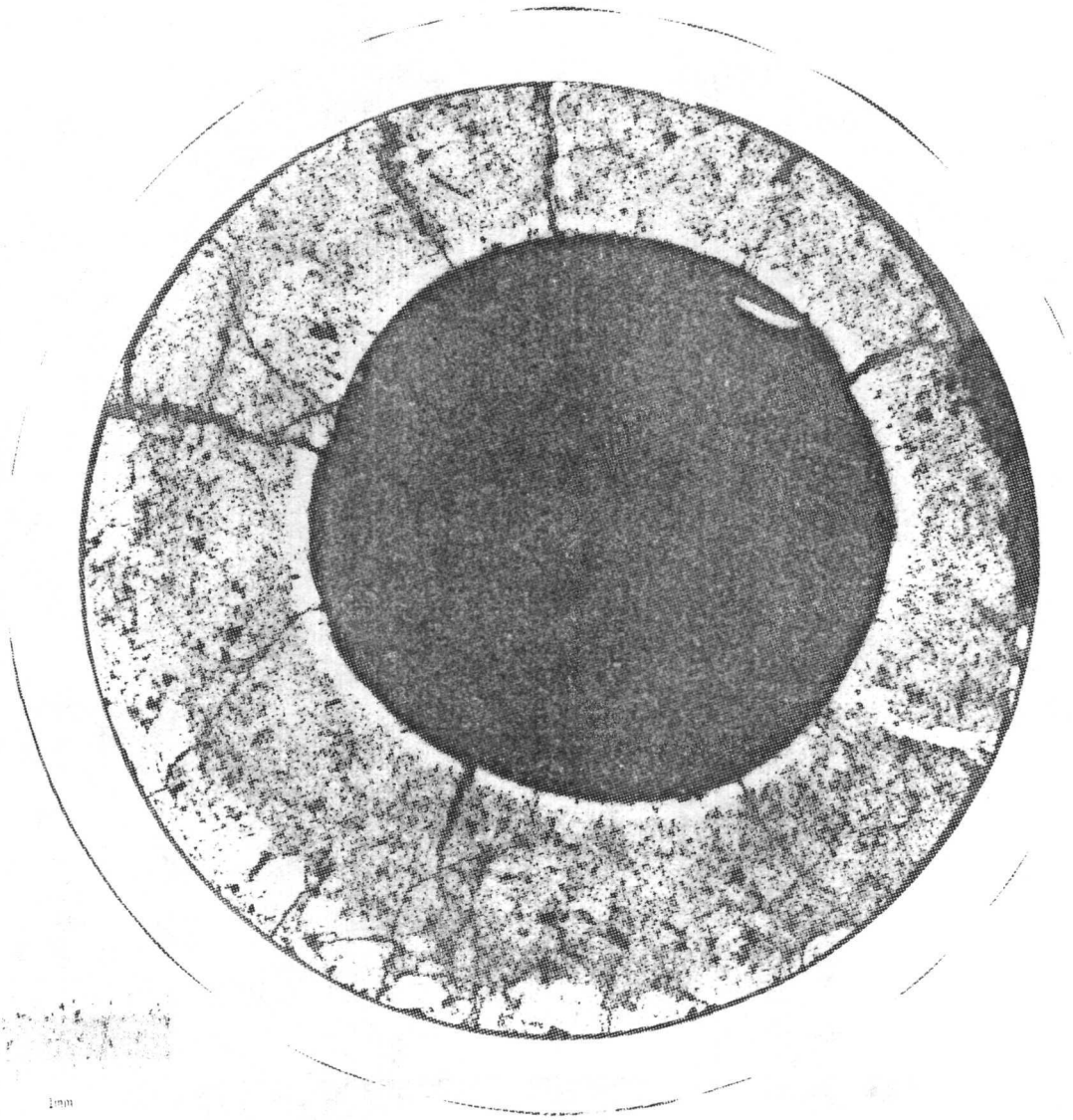

FIGURE 16. Outer Pin Specimen at the 16 cm Level.

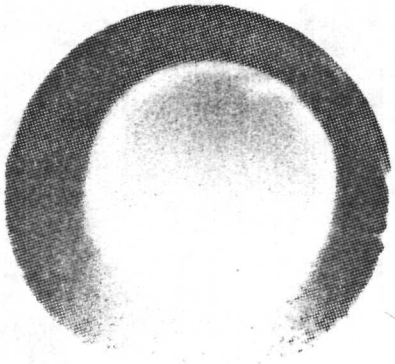

FIGURE 17. Beta-Gamma Autoradiograph of Outer Pin Specimen at the 16 cm Level.

MOLTEN FUEL PENETRATION IN W2-B2

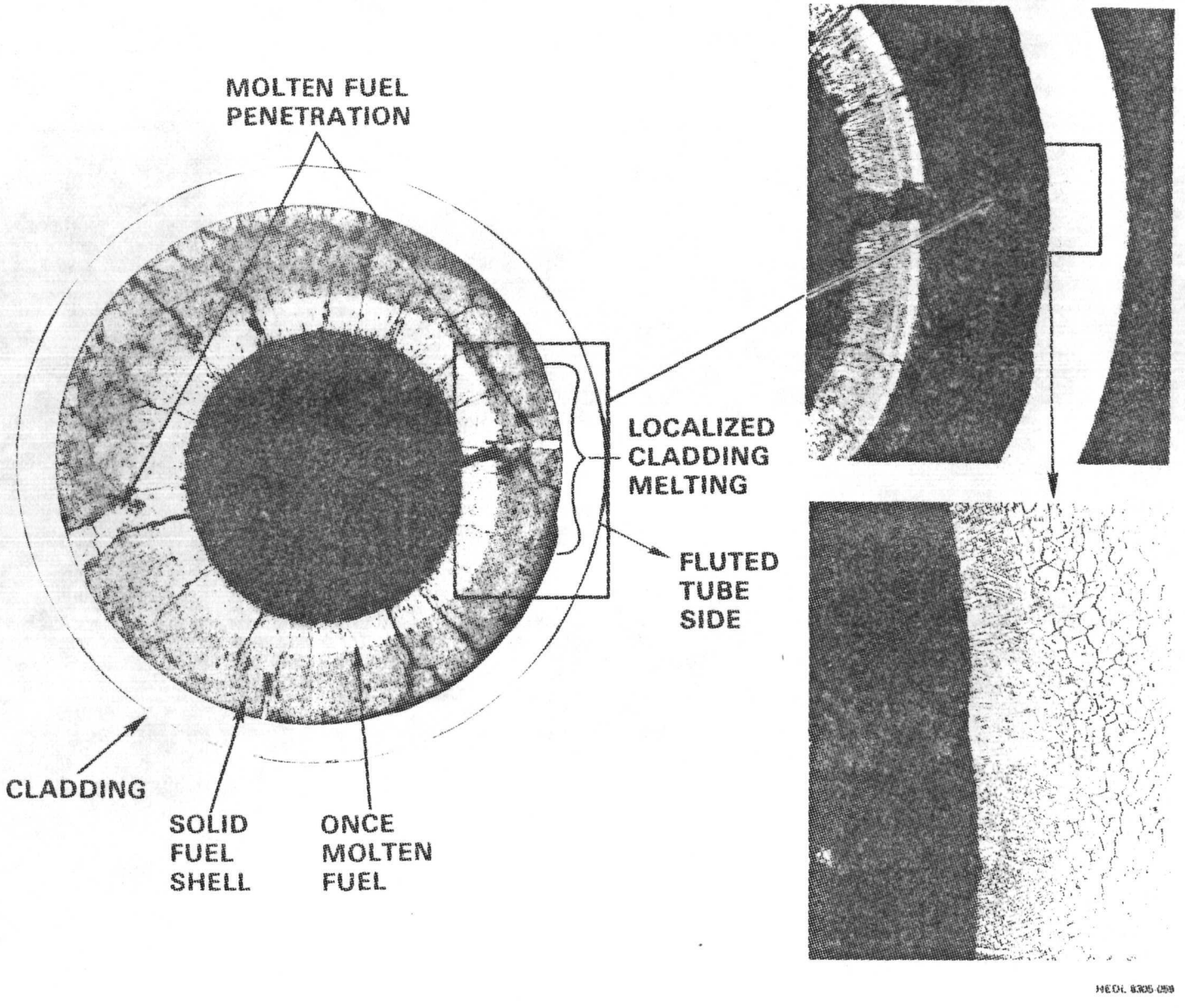

FIGURE 18. Molten Fuel Penetration and Cladding Melting in an Outer Pin Specimen at the 39 cm Level.

Summary

POST-TEST EXAMINATION OBSERVATIONS FOR THE W-2 SLSF EXPERIMENT

A. L. Pitner, D. E. Smith, G. E. Culley
Westinghouse Hanford Company
Hanford Engineering Development Laboratory
Richland, Washington

The W-2 experiment was conducted in the Sodium Loop Safety Facility (SLSF) to characterize the failure response of full-length, preconditioned LMFBR fuel pins subjected to slow (5¢/s) unprotected transient overpower (TOP) conditions.[1,2] Disruptive failure of the 7-pin test bundle occurred at 3.2 times the nominal power level as predicted, but at an axial midplane location rather than the expected upper third level in the center pin. The objectives of the post-test examination (PTE) were to characterize the physical condition of the test assembly following the disruptive failure, and identify any specific circumstances that may have contributed to the unexpected midplane failure response.

Post-transient neutron radiography[1] and post-test disassembly revealed that all seven test pins were severely disrupted over the central ~10 cm section of the test bundle, and that substantial quantities of molten fuel had moved from both ends of the pins and out the midplane failure location into the coolant channels. The lower portions of the fuel pins remained intact and in good condition except for some residual bowing. Above the axial midplane failure region, essentially all of the cladding was melted away, but the individual fuel columns in the upper region remained intact and retained a bundle-type configuration. Thus, the overall nature of the failure event was interpreted to be relatively mild.

A typical post-test configuration of the upper test bundle is shown in Figure 1, which is a transverse view at the 70 cm above bottom of fuel column level. The fuel pellets generally had large central voids where molten fuel had escaped,

and fuel and cladding residue were interspersed in the flow channels. It is estimated that about one-third of the fuel inventory was expelled during the TOP event.

Gamma scanning of test components was performed to characterize the axial power profile along the test bundle. The results indicated that the peak-to-average power ratio was 1.39, rather than 1.25 as expected from pretest analyses and critical facility measurements. The implication of this finding was that thermal flux levels near the axial midplane were higher than expected. Accordingly, power densities in the fuel at midplane were greater and skewed more radially outward than calculated in pretest analyses, and fuel melting behavior in the test pins reflected this situation.

Figure 2 shows a transverse metallography specimen taken at the 39 cm level. Several instances of molten fuel penetration of the solid outer fuel shell and contact with the cladding are apparent. On the fluted tube side of the pin, where pin bowing-induced flow restrictions are believed to have caused high cladding temperatures, molten fuel penetration caused localized melting of the cladding inner surface in the vicinity of the contact point. This phenomenon is believed responsible for the initial disruptive pin failure at the axial midplane.

Based on PTE observations, the W-2 failure event was characterized as relatively non-violent in nature. The measured axial power profile and metallographic examination results provided key input into interpreting the cause of the unexpected midplane failure. Conditions responsible for the W-2 midplane failure were unique to the experiment, and would not be operative in full size LMFBR fuel assemblies.

References

1. J. M. Henderson, et.al., Fuel Pin Behavior Under Slow Overpower Transient Conditions; HEDL W-2 Experiment Results, Proc. ANS Top Mtg. on Reactor Safety Aspects of Fuel Behavior, pp. 2-67 - 2-78, Sun Valley, Idaho, August 2-6, 1981.

2. D. E. Smith, et.al., Post-Test Analysis of the W-2 SLSF Experiment, ANS Transactions, 44, p. 225 (1983).

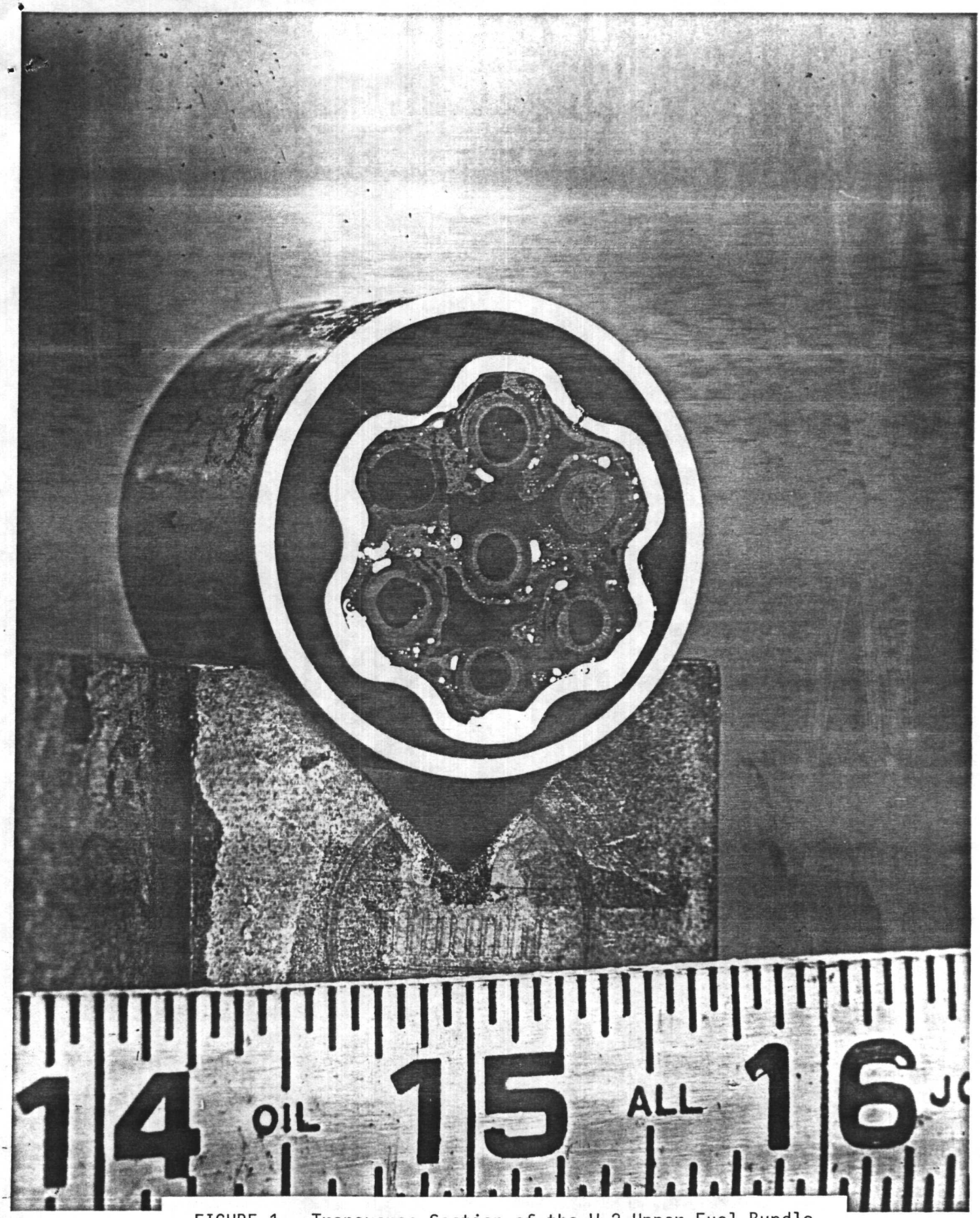

FIGURE 1. Transverse Section of the W-2 Upper Fuel Bundle.

MOLTEN FUEL PENETRATION IN W2-B2

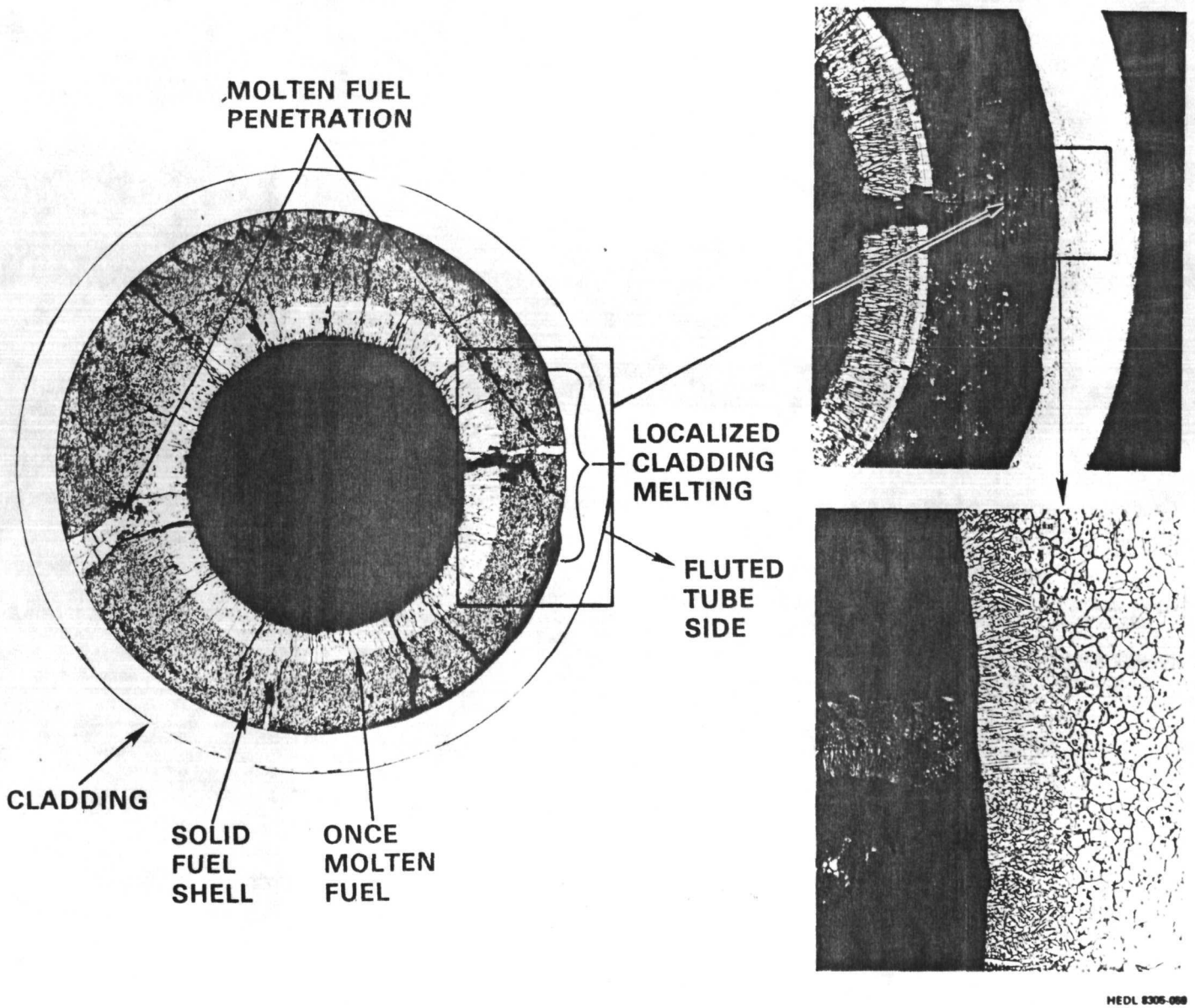

FIGURE 2. Molten Fuel Penetration and Local Cladding Melting in a W-2 Outer Fuel Pin.